

# A Command Preprocessor for Antenna Motion without Overshoots

W. Gawronski<sup>1</sup>

*In order to ensure smooth and stable antenna motion, the DSN antennas are commanded by the command preprocessor (CPP). The preprocessed command generated by the CPP prevents the antenna from jerking and limit cycling, but it is not designed to move the antenna without overshoots during position offsets, acquisition of targets, or slewing (the antenna overshoots if its position exceeds the commanded position before approaching the commanded position). It is desirable to reduce or eliminate overshoots since they increase the acquisition time and may cause damage while moving the antenna to the stow position or when approaching the cable-wrap limits. The article presents an upgrade of the existing CPP such that antenna overshoots are negligibly small and the acquisition time is close to the optimal.*

## I. Introduction

The command preprocessor (CPP), as presented in [1], is used by the DSN antennas to improve tracking and slewing motions. The CPP was designed to ensure smooth and stable antenna motion without limit cycling. However, these improvements do not prevent overshoots of the CPP and of the antenna during position offsets, acquisition of targets, or slewing; an overshoot is an antenna position that exceeds the commanded position before approaching the commanded position. It is recommended that overshoots be reduced or eliminated since they increase the acquisition time and may cause damage when moving the antenna to the stow position or when approaching clockwise or counter-clockwise limits of the cable wrap. This article introduces two upgrades of the existing CPP that reduce or eliminate overshoots of the 34-meter and 70-meter antennas. The first one includes the modification of the CPP gain to eliminate the CPP overshoots. The second upgrade includes the addition of a derivative gain to the CPP to eliminate the antenna overshoots.

## II. Description of the Current CPP

Antenna motions are limited in the sense that the rates and acceleration cannot exceed the imposed limits. For example, the rate limit of the beam-waveguide (BWG) antenna is 0.8 deg/s, and the acceleration limit is 0.4 deg/s<sup>2</sup>. The rate and acceleration limits may cause antenna uncontrolled oscillations

---

<sup>1</sup> Communications Ground Systems Section.

The research described in this publication was carried out by the Jet Propulsion Laboratory, California Institute of Technology, under a contract with the National Aeronautics and Space Administration.

(so-called limit cycling) if no additional measures are taken. One way to prevent limit cycling is to implement a nonlinear device—the preprocessor (as described in [1]). It is a part of the antenna control system, and its location within the system is shown in Fig. 1. In this figure,  $r$  is the original command,  $r_p$  is the preprocessed command,  $u$  is the controller output, and  $y$  is the antenna position.

The CPP is an algorithm that generates a modified command to an antenna. The modified command is identical to the original one if the rate and accelerations of the original command are within the limits; when the limits are met or violated, a command rate and acceleration are close to their maximal (or minimal) values. The block diagram of the current CPP algorithm (as presented in [1]) is shown in Fig. 2 (thin line). It was tested and is implemented at the BWG antennas. The CPP concept is similar to the antenna control system. In fact, it is a software imitation of the antenna control system, where an integrator replaces the antenna model. Besides the integrator, the CPP also includes the rate and acceleration limiters and a controller. The latter consists of the feedforward part and a proportional feedback with a variable gain denoted  $k_{pi}$ . The CPP is a discrete-time system, with sampling time  $T = 0.02$  s or, more recently, with  $T = 0.04$  s. The command at the time instant  $iT$  is denoted  $r_i$ ; the preprocessed command at the same instant is denoted  $r_{pi}$ ; the input to the integrator is  $u_i$ ; the preprocessor error is  $e_i = r_i - r_{pi}$ ; and its derivative is  $e_{di}$ . The rate limit is  $v_{\max} = 0.8$  deg/s for 34-m antennas and 0.25 deg/s for 70-m antennas; the acceleration limit is  $a_{\max} = 0.4$  deg/s<sup>2</sup> for 34-m antennas and 0.2 deg/s<sup>2</sup> for 70-m antennas.

The gain  $k_{pi}$  depends on the preprocessor error  $e_i$ , and, at the  $i$ th time instant  $t = iT$ , it is

$$k_{pi} = k_o + k_v e^{-\beta|e_i|} \quad (1)$$

where  $k_o$  is the constant part of the gain,  $k_v$  is the gain of the variable part, and  $\beta$  is the gain exponential. In [1] the following CPP parameters were chosen:  $k_o = 1$ ,  $k_v = 5$ , and  $\beta = 20$ . The plot of  $k_{pi}(e_i)$  for these parameters is given by the solid line in Fig. 3.



Fig. 1. Antenna with CPP.

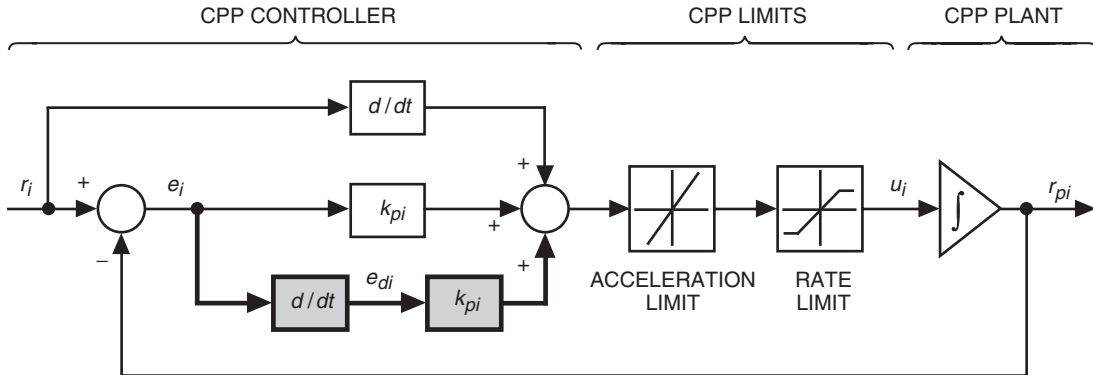


Fig. 2. Current CPP (thin line) and its upgrade (thick line).

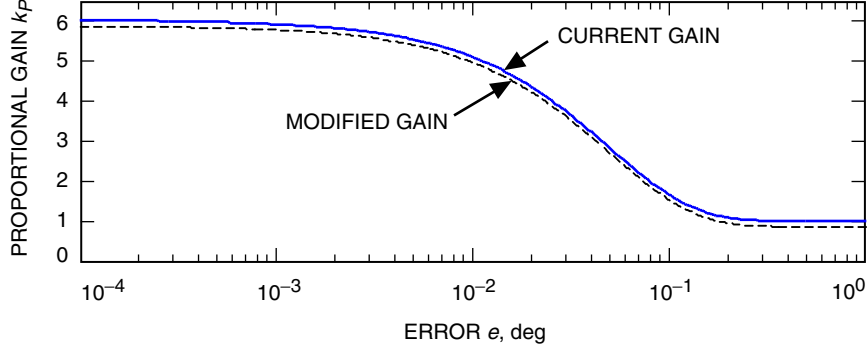


Fig. 3. CPP proportional gain versus CPP error.

The antenna operations include tracking and non-tracking activities. During tracking, when the rate and acceleration limits are not violated, the preprocessed command is identical to the original command. Non-tracking activities consist of applying engineering test signals, slewing, and target acquisition. Antenna slews and targets are acquired by inserting step commands. For this reason, we chose step inputs as tools to evaluate the CPP performance. Two kinds of steps are selected: small steps (that do not violate the rate and acceleration limits) and large steps (that violate the limits). For the antenna sampling time  $T = 0.04$  s and the rate limit  $v_{\max} = 0.8$  deg/s, the maximal step that does not violate the rate limit is  $v_{\max}T = 0.032$  deg. Thus, a step of 0.01 deg is considered small, and one of 10 deg is considered large. The plot of the CPP response to a 0.01-deg step command (in Fig. 4) shows a settling time of 0.75 s and no overshoot. However, the CPP response to a 10-deg step (the dashed lines in Fig. 5) shows an overshoot of about 100 mdeg. The purpose of the following section is to eliminate the CPP overshoots at large steps.

### III. CPP with No Overshoots

For antenna operational purposes, it is preferable that the CPP not have overshoots for large as well as for small steps. Overshoots appear during the deceleration phase of the step response. They depend on the CPP gain  $k_o$  [as in Eq. (1)]. We assumed the CPP acceleration limit is 0.9 of the antenna acceleration limit ( $0.9a_{\max} = 0.72$  deg/s<sup>2</sup>), and we simulated the CPP large-step responses for values of  $k_o$  from 0.8 to 1.0 and for different step amplitudes—from 5 to 9 deg. The plot of the overshoot values for large steps with respect to  $k_o$  is shown in Fig. 6. The figure shows that, for gain  $k_o < 0.885$ , the overshoot disappeared. We chose  $k_o = 0.88$ , the gain that does not produce overshoots. Indeed, it was verified with the simulation of the 10-deg step response, which is shown in Fig. 5 (solid lines).

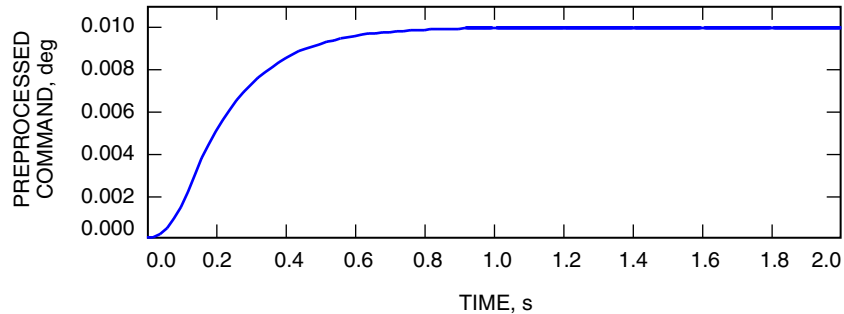
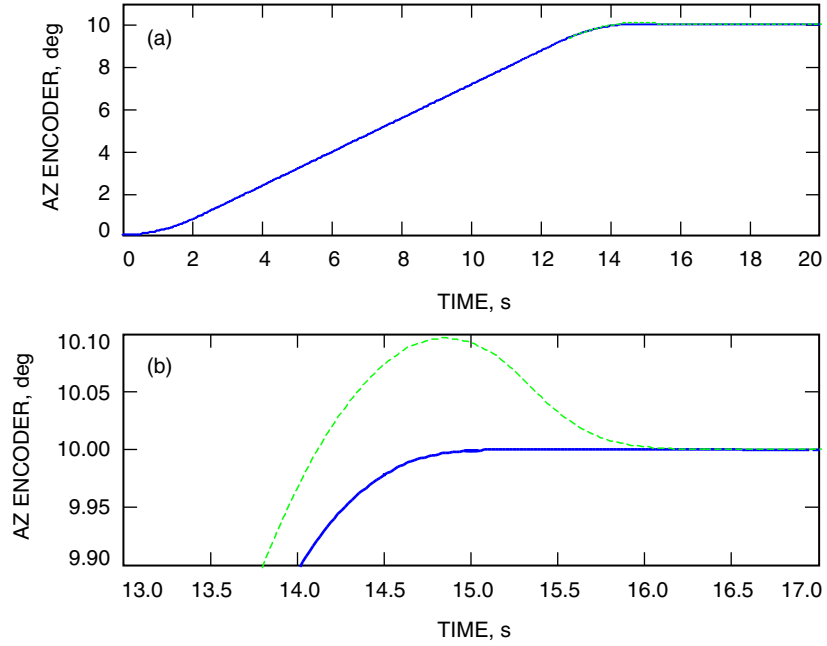
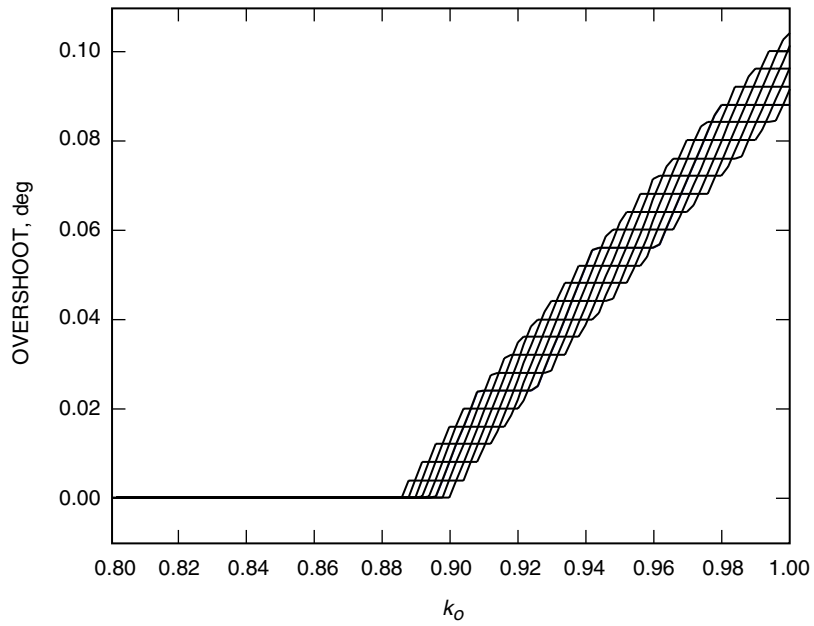


Fig. 4. The current CPP response to a small-step command.



**Fig. 5. The CPP response to a large step for  $k_O = 1.00$  (dashed line) and  $k_O = 0.88$  (solid line): (a) full view and (b) zoomed view.**



**Fig. 6. CPP overshoots for various large steps versus CPP gain  $k_O$ , and for the acceleration limit of  $0.72 \text{ deg/s}^2$ .**

#### IV. CPP with No Overshoots of the 34-m Antenna

Although overshoots are absent in the CPP step responses, the antenna response to the no-overshoot CPP command still showed overshoots for both small and large steps. This can be seen in Figs. 7 and 8 for the case of  $k_d = 0$ . The purpose of the remaining portion of this article is to modify the CPP such that the antenna overshoots are reduced or eliminated.

##### A. A Simple CPP Upgrade

The overshoots can be reduced or eliminated by introduction of the derivative feedback in the CPP; the feedback is shown by the thick line in Fig. 2. The CPP derivative gain  $k_d$  reduces (and a large enough

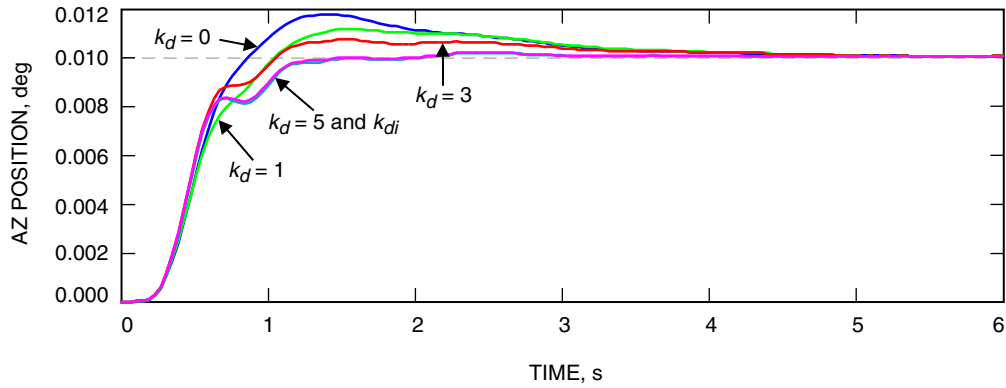


Fig. 7. Antenna response to a 0.01-deg step for CPP derivative gains  $k_d = 0, 1, 3,$  and  $5$  and for variable derivative gain  $k_{dj}$ .

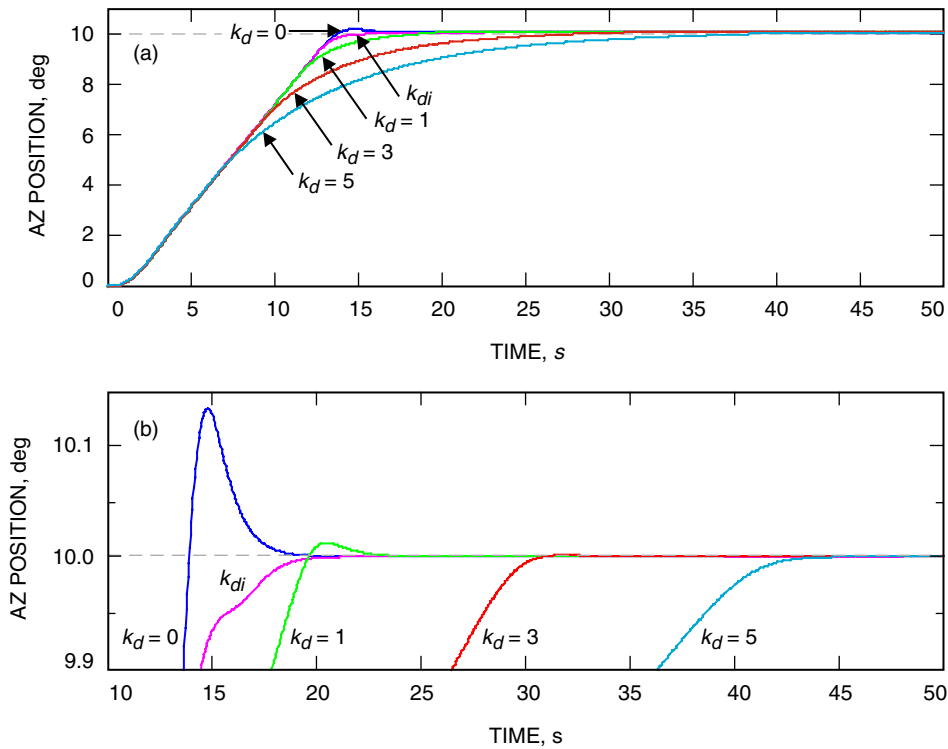


Fig. 8. Antenna response to a 10-deg step for CPP derivative gains  $k_d = 0, 1, 3,$  and  $5$  and for variable derivative gain  $k_{dj}$ : (a) full view and (b) zoomed view.

gain  $k_d$  eliminates) *antenna* overshoots for small and large steps. The plots of the DSS-25 antenna responses to a 10-mdeg step in azimuth (AZ) are shown in Fig. 7 for  $k_d = 0, 1, 3,$  and  $5$ . Indeed, the increase of the derivative gain reduces the overshoot, until it disappears for  $k_d = 5$ . For large steps (3 deg and larger), the overshoot also decreases with the increased value of the CPP derivative gain. This is seen in Fig. 8 in the antenna responses to a step of 10 deg. However, the major drawback of this approach is the increased settling time. It increases with the increase of the derivative gain, about 5 s per unit of the gain. The increased settling time led us to additional adjustments of the CPP in order to improve its performance.

## B. An Advanced CPP Upgrade

In the following, we show that we can eliminate the overshoot without expanding the settling time by introducing a variable gain of the derivative feedback. The variable derivative gain depends on the derivative (or rate) of the CPP error  $e_{di}$  basic

$$k_{di} = k_{do} + k_{dv}e^{-\beta_d|e_{di}|} \quad (2)$$

This gain is similar to the variable proportional gain [see Eq. (1)]. The parameter values in this equation are  $k_{do} = 0.25$ ,  $k_{dv} = 5.0$ , and  $\beta_d = 20$ . The plot of  $k_{di}$  versus  $e_{di}$  is shown in Fig. 9, and the parameters are given in Table 1.

Simulations for small and large steps were conducted to illustrate the performance of the antenna with the variable derivative gain of the CPP. The small-step responses of the antenna with an unmodified CPP (i.e., for  $k_d = 0$ ) and with variable gain  $k_{di}$  are shown in Fig. 7. The figure shows practically nonexistent overshoot for variable gain  $k_{di}$ . However, the small-step response shows a jerk at the CPP output for  $t = 0.2$  to  $0.5$  s (see Fig. 10). Note that the largest jerk appears for the step of amplitude 10 mdeg (see Fig. 11). Larger and smaller steps produce smaller jerks or no jerk at all. The antenna response to

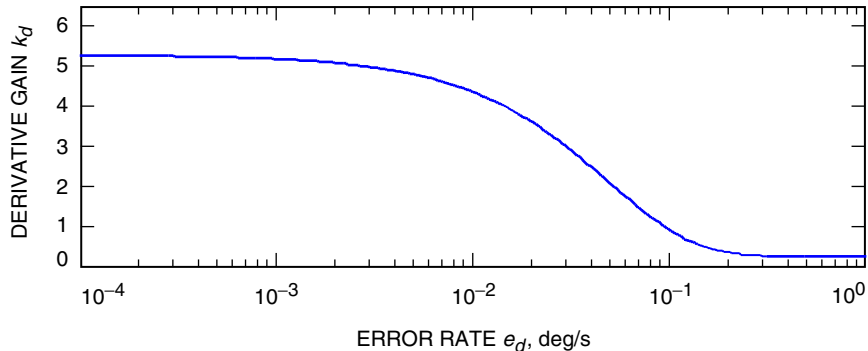
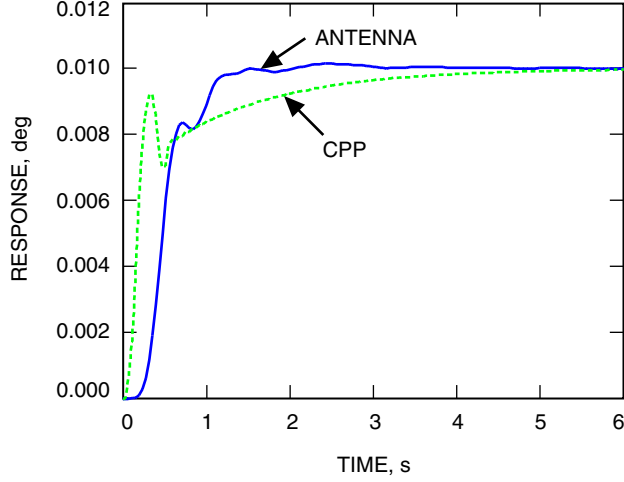


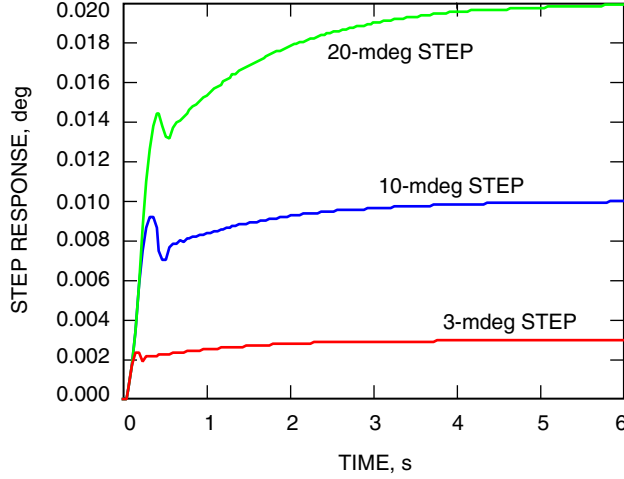
Fig. 9. Derivative CPP gain versus CPP error rate.

Table 1. Parameters of the CPP and ME controller for 34-meter and 70-meter antennas.

Antenna	CPP proportional gain			CPP derivative gain			ME	
	$k_o$	$k_v$	$\beta$	$k_{do}$	$k_{dv}$	$\beta_d$	$k_p$	$k_i$
34 m	0.88	5.0	20	0.25	5.0	20	—	—
70 m, AC mode	0.70	5.0	30	0.0	5.0	30	4.0	2.5
70 m, MEE mode	0.70	5.0	30	0.0	5.0	30	10.0	4.0



**Fig. 10. Responses of the variable gain CPP and the antenna to a 0.01-deg step.**



**Fig. 11. CPP responses to 3-, 10-, and 20-mdeg steps.**

the CPP jerk is less dramatic. Nevertheless, it should be verified in the field if this phenomenon has a significant impact on the antenna dynamics.

The large-step antenna responses are shown in Fig. 8 for the antenna with CPP variable derivative gain. The plots show no overshoot and also no increase in the settling time.

Finally, in Fig. 12 we compare the CPP rates and accelerations for the current CPP (i.e., with  $k_d = 0$ ), for the CPP with no overshoot ( $k_d = 5$ ), and for the CPP with the variable gain  $k_d$ . The plots show that the current CPP is fast: it starts the motion with full acceleration, moves on at full speed, and decelerates with almost full deceleration. But this produces overshoot of an antenna. The modified CPP also starts with full acceleration, moves on at full speed to a certain moment only, and slowly decelerates with partial allowed deceleration. It produces no overshoot, but it is much slower than the current CPP. The variable-gain CPP is fast at the start, moving with full acceleration at the beginning, moving on at full speed, and decelerating with almost full deceleration. But, it produces no overshoot of the antenna. The difference between the first and the latter CPP lies in “smarter” deceleration, which starts a little later for the variable-gain CPP but finishes faster than the current CPP.

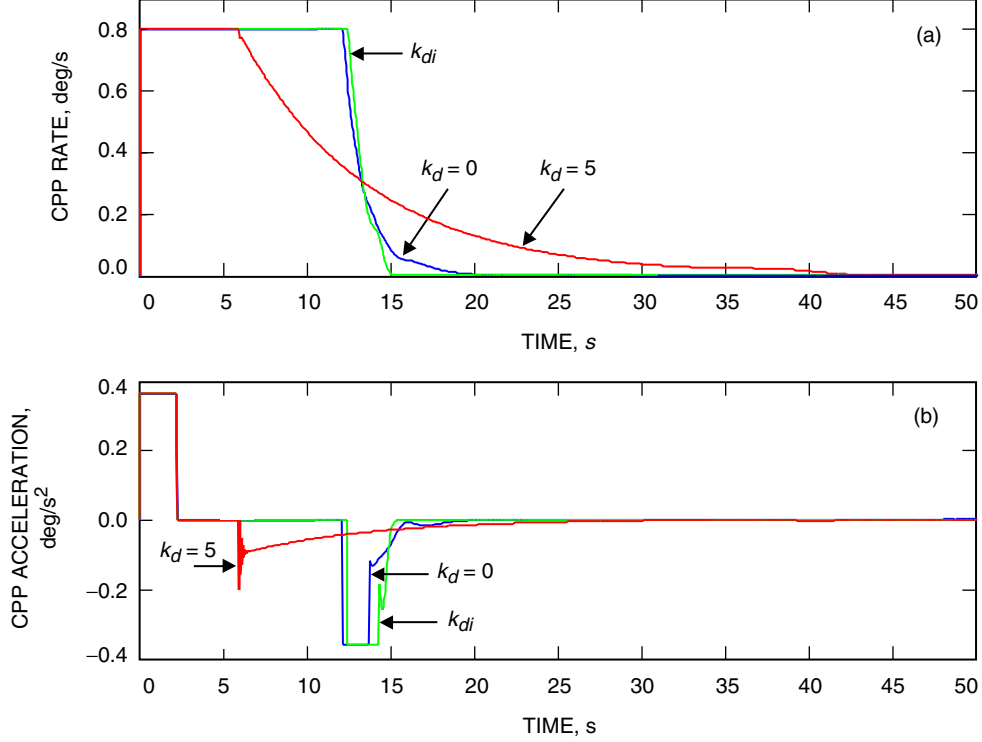


Fig. 12. The current CPP,  $k_d=0$ , the CPP with constant derivative,  $k_d=5$ , and the CPP with variable derivative gain,  $k_{dj}$ : (a) rates and (b) accelerations.

## V. CPP with No Overshoots of the 70-m Antenna

The 70-meter antenna control system is different from that of the 34-meter antenna. It consists of the master equatorial (ME) control system and the control system of the antenna itself. Both systems are connected by the autocollimator, as shown in Fig. 13, where  $r$  is the command,  $r_p$  is the preprocessed command,  $e_a$  is the autocollimator error,  $u$  is the antenna rate command,  $y$  is the antenna position, and  $u_{me}$  is the ME rate command. The configuration of these two systems is called the autocollimator (AC) mode. In this mode, the ME follows the command, and the antenna follows the ME: the autocollimator compares the ME position with the antenna position and creates the position error that closes the antenna feedback loop. The arrangement of the antenna and ME can be reversed, as shown in Fig. 14, where the antenna follows the command and the ME follows the antenna, again using the autocollimator. This mode is called the ME encoder (MEE) mode. In the next subsection, we analyze the CPP design that does not cause overshoots of the 70-m antenna in either the AC mode or the MEE mode.

### A. AC Mode

In this mode, when the antenna (and ME) are not close to the ME keyhole, the preprocessed command  $r_p$  from the antenna command preprocessor is used both by the ME and by the antenna (see Fig. 13). If the antenna and ME are close to the ME keyhole, the ME switches to its own CPP in order to move at its maximal rate rather than at the antenna maximal rate. The rate limit for the antenna is  $v_{\max} = 0.25$  deg/s, and the acceleration limit is  $a_{\max} = 0.2$  deg/s<sup>2</sup>. The rate limit for the ME is  $v_{\max} = 2.0$  deg/s, and the acceleration limit is  $a_{\max} = 1.6$  deg/s<sup>2</sup>. The ME proportional gain is  $k_{pme} = 4$ , and the integral gain is  $k_{ime} = 2.5$ , as shown in Table 1.

The CPP is shown in Fig. 2. Its proportional gain  $k_{pi}$  depends on the preprocessor error  $e_i$ ; at the  $i$ th time instant  $t = iT$ , it is as in Eq. (1), with  $k_o = 0.7$ ,  $k_v = 5$ , and  $\beta = 30$  (see Table 1). We simulated two



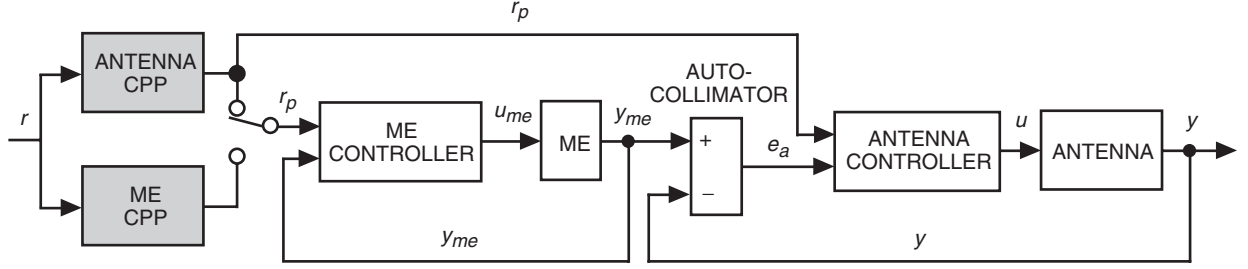


Fig. 13. AC mode of the 70-meter antenna control system.

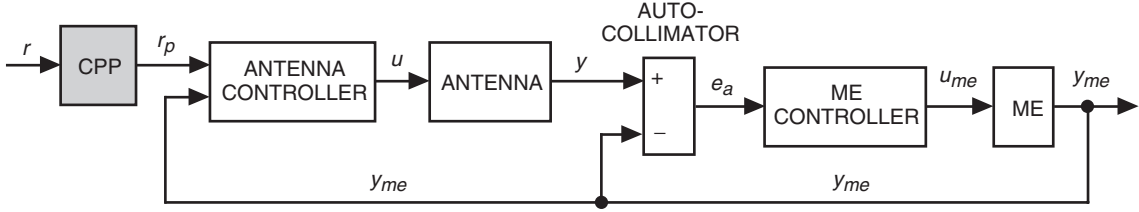


Fig. 14. MEE mode of the 70-meter antenna control system.

cases: the constant and variable derivative gain of the CPP, the latter as in Eq. (2). We assumed constant gain  $k_d$  to be 0, 1, 3, or 5, and we simulated small- and large-step responses. The small-step responses are shown in Fig. 15, where one can see that increased  $k_d$  gain reduces the overshoot that eventually disappears for  $k_d = 5$ . The large-step responses are shown in Figs. 16(a) and 16(b), where again the increased derivative gain reduces the overshoot that disappears for  $k_d = 5$ , but the overshoot reduction increases settling time by 25 s for the  $k_d = 5$  case as compared with the  $k_d = 0$  case. This drawback can be eliminated by applying the variable derivative gain that depends on the absolute value of the error rate, as in Eq. (2); the gain is large ( $k_{di} = 5$ ) for a small error rate, and small ( $k_{di}$  approaching zero) for a large error rate. The parameters of the derivative gain are  $k_{do} = 0$ ,  $k_{dv} = 5$ , and  $\beta_d = 30$ . The responses of the antenna in the AC mode with a variable-gain CPP for small steps are shown in Fig. 15, and in Fig. 16 for large steps. Both figures show no overshoot; moreover, the large-step response shows no increase in the settling time.

## B. MEE Mode

In this mode, the preprocessed command  $r_p$  is used only by the antenna (see Fig. 14). The analysis for the MEE mode is similar to that for the AC mode. The parameters of the derivative gain are the same as for the AC mode, except those for the ME gain, which were modified; in the MEE mode, the ME proportional gain is  $k_{pme} = 10$ , and the ME integral gain is  $k_{ime} = 4$ , see Table 1. The results for small and large steps for the CPP with constant derivative gain are identical to those for the AC mode, as shown in Figs. 15 and 16. The results for the small steps and large steps for the CPP with variable derivative gain also are identical to those for the AC mode shown in Figs. 15 and 16. All of these figures show no overshoot and no increase in settling time.

## VI. The Derivative Algorithm for the CPP

The added feedback of the proposed CPP uses the derivative (rate)  $e_{di}$  of the CPP error  $e_i$ . Conventionally, the rate is computed as follows:

$$e_{di} = \frac{e_i - e_{i-1}}{T} \quad (3)$$

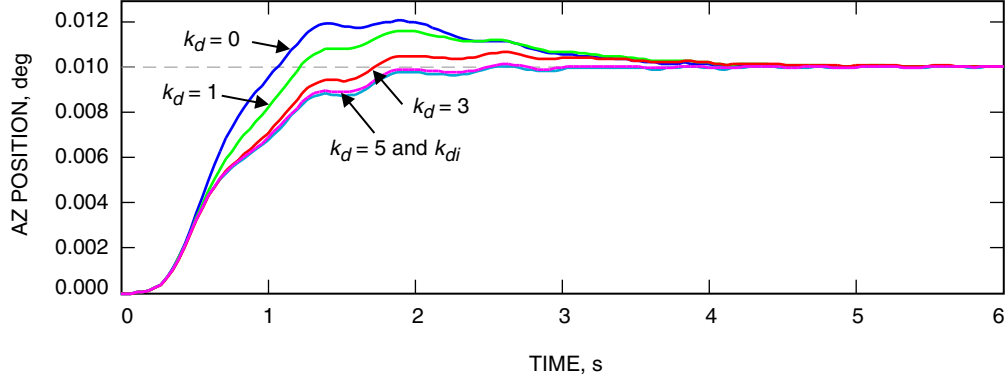


**Fig. 15. Small-step responses of the 70-meter antenna (AC and MEE modes) for CPP derivative gains of 0, 1, 3, and 5 and for the CPP with variable derivative gain  $k_{dj}$ .**

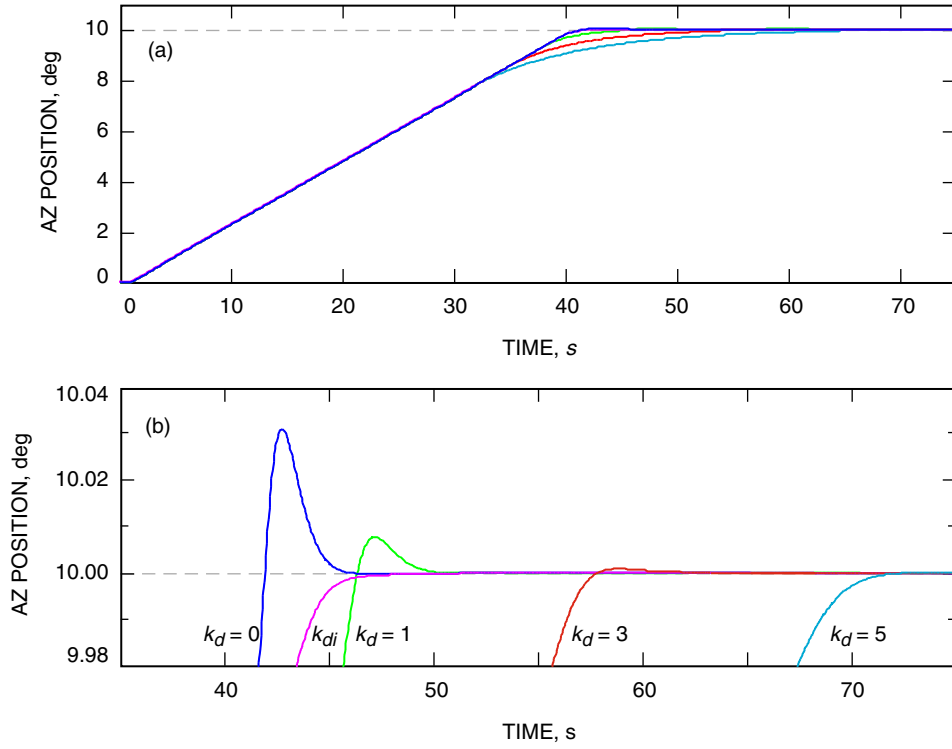


**Fig. 16. Large-step responses of the 70-meter antenna (AC and MEE modes) for CPP derivative gains of 0, 1, 3, and 5 and for the CPP with variable derivative gain  $k_{dj}$ : (a) full view and (b) zoomed view.**

which can be accomplished by using the following digital filter:

$$F(z) = \frac{z - 1}{Tz} \quad (4)$$

It was observed, however, that the filter causes an unacceptable steady-state error of the CPP. In order to eliminate the error, we added a low-pass term to the derivative filter, which corresponds to the following continuous-time transfer function:

$$F(s) = \frac{s}{\tau s + 1} \quad (5)$$

The filter time constant,  $\tau$ , was chosen to be  $\tau = 0.14$  s for the sampling time  $T = 0.04$  s and  $\tau = 0.10$  s for the sampling time  $T = 0.02$  s. The corresponding digital filters are

$$F(z) = \frac{b(z - 1)}{z - a} \quad (6)$$

where  $a = 0.75148$  for  $T = 0.04$  and  $a = 0.81873$  for  $T = 0.02$  s, while  $b = 7.14286$  for  $T = 0.04$  s and  $b = 10$  for  $T = 0.02$  s. The parameters are collected in Table 2. The time-domain equation that corresponds to the filter is as follows:

$$e_{di} = ae_{di-1} + be_i - be_{i-1} \quad (7)$$

Equation (7) will be implemented in the antenna controller software.

**Table 2. Parameters  $a, b$  for 25-Hz and 50-Hz sampling frequencies.**

Sampling frequency, Hz	$a$	$b$
25	0.75148	7.14229
50	0.81873	10.0000

## VII. Conclusions

The article presents two upgrades of the existing CPP to improve the antenna motion while tracking, acquiring targets, and slewing. The first one—a change in the CPP proportional gain—eliminates the CPP overshoots. The second one—an addition of the derivative feedback in the CPP—eliminates the antenna overshoots. The constant derivative gain reduces or eliminates the antenna overshoots but increases the settling time. The variable derivative gain eliminates the antenna overshoots without increasing the settling time. The implementation of the latter should not be difficult, since the variations of the derivative gain are similar to the variations of the proportional gain, which is already implemented. The analysis was performed for the 34-meter antennas (such as the high-efficiency and BWG antennas) and for the 70-meter antennas in the AC and MEE modes.

## Reference

- [1] W. Gawronski, “Command Preprocessor for the Beam-Waveguide Antennas,” *The Telecommunications and Mission Operations Progress Report 42-136, October–December 1998*, Jet Propulsion Laboratory, Pasadena, California, pp. 1–10, February 15, 1999.  
[http://tmo.jpl.nasa.gov/tmo/progress\\_report/42-136/136A.pdf](http://tmo.jpl.nasa.gov/tmo/progress_report/42-136/136A.pdf)